CHIN. PHYS. LETT. Vol. 38, No. 10 (2021) 106101

Observation of the Pinning-Induced Crystal-Hexatic-Glass Transition in Two-Dimensional Colloidal Suspensions

Xiaoyan Sun(孙晓燕)[1,2†], Huaguang Wang(王华光)[2†], Hao Feng(冯浩)[3], Zexin Zhang(张泽新)[2,3*], and Yuqiang Ma(马余强)[4*]

[1]*Department of Optoelectronics and Energy Engineering, City College of Suzhou, Suzhou 215104, China*
[2]*College of Chemistry, Chemical Engineering and Materials Science, Soochow University, Suzhou 215123, China*
[3]*Center for Soft Condensed Matter Physics and Interdisciplinary Research, Soochow University, Suzhou 215006, China*
[4]*National Laboratory of Solid State Microstructures and Department of Physics, Nanjing University, Nanjing 210093, China*

(Received 21 July 2021; accepted 20 August 2021; published online 18 September 2021)

Identification of the glass formation process in various conditions is of importance for fundamental understanding of the mechanism of glass transitions as well as for developments and applications of glassy materials. We investigate the role of pinning in driving the transformation of crystal into glass in two-dimensional colloidal suspensions of monodisperse microspheres. The pinning is produced by immobilizing a fraction of microspheres on the substrate of sample cells where the mobile microspheres sediment. Structurally, the crystal-hexatic-glass transition occurs with increasing the number fraction of pinning ρ_{pinning}, and the orientational correlation exhibits a change from quasi-long-range to short-range order at $\rho_{\text{pinning}} = 0.02$. Interestingly, the dynamics shows a non-monotonic change with increasing the fraction of pinning. This is due to the competition between the disorder that enhances the dynamics and the pinning that hinders the particle motions. Our work highlights the important role of the pinning on the colloidal glass transition, which not only provides a new strategy to prevent crystallization forming glass, but also is helpful for understanding of the vitrification in colloidal systems.

DOI: 10.1088/0256-307X/38/10/106101

Disorder and order play crucial roles in crystallization, melting and glass transition. In a crystal-to-liquid transition, both the orientational and translational order are lost, and the relaxation time dramatically decreases.[1] Conversely, in a liquid-to-glass transition, although the relaxation time increases dramatically, the orientational and translational orders experience no apparent change. Such a lack of significant correlation between order, disorder, and dynamics makes the glass transition one of the most interesting, unsolved research problems in condensed matter physics.[2–4] Nevertheless, disorder is the key structural signature in the formation of glass from crystal phase. Compared with order, disorder is an interesting yet much less studied counterpart. Usually, disorder is induced by adding particles with a different size to an otherwise monodispersed colloidal system, and a crystal-to-glass transition has been observed.[5] Here, we propose a new way of introducing disorder by random pinning in colloidal suspensions, and explore the crystal-to-glass transition. The random pinning is formed by pinning a subset of colloidal particles with random positions, and thus the properties of the remaining, unpinned particles, are investigated. This pinning concept has recently attracted widespread interest in other contexts, i.e. to study structures and dynamics near the glass transition, both theoretically and by computer simulations.[6,7] For example, computer simulations have shown that random pinning can slow down dynamics dramatically,[6,8] and induce a liquid-to-glass transition.[9–11] Moreover, it has been found by large scale simulations that the relaxation dynamics of glass-forming liquids depend on the pinning fraction exponentially.[12] However, the experimental study of such random pinning affecting the structures and dynamics remains rare.

In this Letter, we design a new colloidal model system where pinning could be systematically adjusted, and study the effect of the pinning on the structures and dynamics with single-particle resolution by video microscopy. The number fraction of the pinning (ρ_{pinning}) is varied from 0 to 0.38 and the area fractions of the suspensions are fixed on nearly 0.84, which is the maximum area fraction we could manage in the current experiments. Transitions from crystal to hexatic and then to glass are observed, which are quantitatively analyzed by a variety of structural and dynamical properties. Similar to the 2D melting,[1,13] the orientational correlation function exhibits a change from quasi-long-range to short-range order across a transition point ($\rho_{\text{pinning}} = 0.02$). Intriguingly, we find that the dynamics shows a non-monotonic dependence on the fraction of the pinning after the transition. This originates from the competition between the disorder that enhances the dynamics and the pinning that hinders the particle motions. Thus the experiments re-

Supported by the National Natural Science Foundation of China (Grant Nos. 12074275, 11704269, and 11704270), the Natural Science Foundation of the Jiangsu Higher Education Institutions of China (Grant Nos. 20KJA150008 and 17KJB140020), and the PAPD Program of Jiangsu Higher Education Institutions.
†These authors contributed equally to this work.
*Corresponding authors. Email: zhangzx@suda.edu.cn; myqiang@nju.edu.cn
© 2021 Chinese Physical Society and IOP Publishing Ltd

veal a critical role of the pinning on the structures and dynamics of colloidal systems, with the pinning triggering the glass formation from crystal and altering the structural relaxation.

In experiment, the pinning was prepared by confining 10 µl of an aqueous colloidal suspension of polystyrene spheres (nominal diameter $\sigma = 3\,\mu$m, Duke Scientific) between two glass coverslips. Then the coverslips were left in a vacuum oven with a temperature of 40 ℃ for 24 h. Because of the solvent evaporation, the particles were stuck on the coverslips. Drying for 2 min on a hot plate at 100 ℃ sinters the particles onto the coverslips. The fraction of the pinning, adjusted by changing the concentration of colloidal suspension, was varied from 0 to 0.38. The fraction is defined as $\rho_{\text{pinning}} = N_{\text{pinning}}/N$, where N_{pinning} and N are the numbers of the pinned particles and total particles in the field of view, respectively. Here the pinning corresponds to particles that stuck on the substrate and cannot move anymore, instead of particles that are trapped by the optical tweezer, in which the particles can still vibrate in the trap.[14–17] The pair correlation function of the pinned particles were measured and the distribution were found to be random (see Fig. S1 in the Supplementary Material).

The sample cell was composed of a glass coverslip with pinning as the bottom wall and a cover glass as the top wall, separated by a plastic ring. The diameter and height of the cell were 6 mm and 5 mm, respectively. After the insertion of suspension of silica microspheres (nominal diameters $\sigma = 3\,\mu$m) with 3 mmol sodium dodecyl sulfate, we sealed the top of the sample cell with a glass coverslip using an epoxy adhesive to prevent contamination of the sample and solvent evaporation. The high mass density of the particles resulted in their sedimentation to the bottom wall and the particles formed a monolayer. During the experiments, it was observed that the particles remained on the bottom wall all time due to the gravity, and the fluctuation of the particle motion in the z-direction was negligible. The ionic strength in the suspension was more than 0.1 mmol and the corresponding Debye screening length was less than 20 nm.[18] Hence the colloidal spheres in the suspension can be considered as hard particles.[19] To realize the crystal to glass transition, we chose to work with concentrated colloidal suspensions at an area fraction of 0.84. Here the area fraction is defined as $\phi = n\pi(\frac{\sigma}{2})^2/A_{\text{T}}$, where n is the number of all particles in the field of view, and A_{T} is the area of the field of view.

After stabilization overnight (∼12 h) on the stage of an inverted microscope (Nikon), no drift flow or packing change was observed in the samples. Then the thermal motions of the colloidal particles were recorded by a CCD camera (Andor) mounted on the microscope at a rate of 3 frames/s. The field of view (FOV) was approximately $390 \times 300\,\mu\text{m}^2$. A standard particle-tracking algorithm was employed to identify the colloidal particle position in video frames.[20] For computing efficiency, we choose a small region ($130 \times 130\,\mu\text{m}^2$, ∼2800 particles) in the center of the FOV to process the data. We verified that the results were not affected by such a procedure.

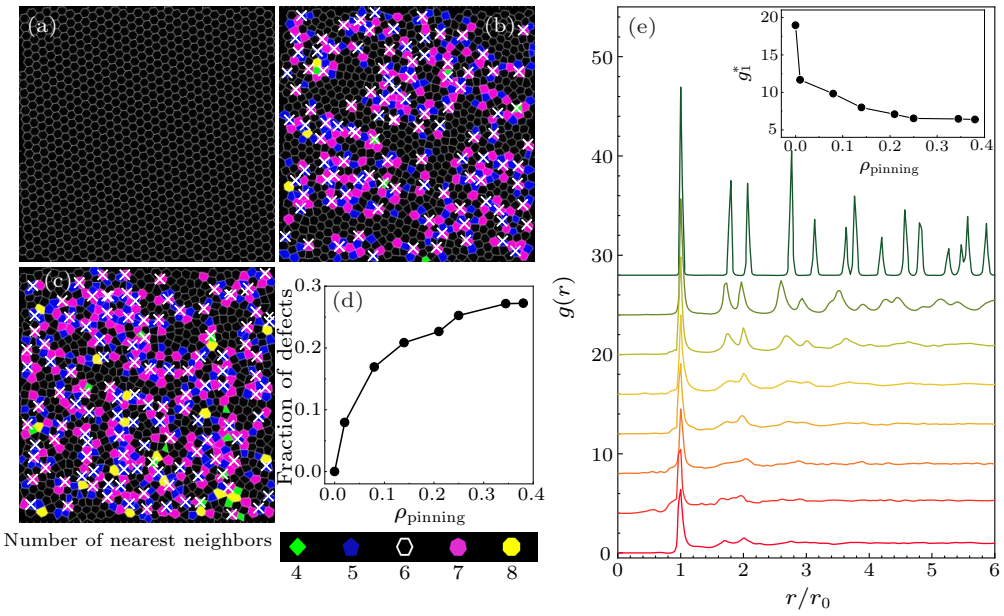

Fig. 1. (a)–(c) The Voronoi constructions of particle configurations at $\rho_{\text{pinning}} = 0$, 0.14, 0.25, respectively. The pinning particles are labeled as cross symbols (×). (d) The fraction of the defects as a function of ρ_{pinning}. (e) Pair correlation function $g(r)$ at different fractions of pinning. The curves are shifted vertically for clarity. Inset: height of the first peak in $g(r)$ as a function of ρ_{pinning}.

To directly visualize the structural change induced by the pinning, the structures are analyzed by the Voronoi diagram shown in Figs. 1(a)–1(c). Without pinning, every particle has six nearest neighbors, representing a crystal phase (Fig. 1(a), note that here the particles vibrate on the crystal lattices and are

not stuck as they may appear). As ρ_{pinning} increases, the number of particles with six nearest neighbors decreases, and the structure becomes more disorder, signifying the glass formation of the system [Figs. 1(b) and 1(c)]. This is confirmed by calculating the fraction of the defects. Here, particles with other than the number of nearest neighbors to be 6 are considered to be defects. As ρ_{pinning} increases, the defect fraction grows gradually, indicating a structural transition due to the pinning-induced disorder [Fig. 1(d)].

The ordering of those different structures is quantified by calculating the pair correlation function: $g(r) = (1/n^2)\langle\rho(r+\Delta r)\rangle\langle\rho(r)\rangle$, where $\rho = \sum_{i=1}^{N(t)}\delta(r - r_i(t))$ is the distribution of particles in the field of view and n is the number fraction of the particles. The angular brackets denote an average over time and space. Figure 1(e) shows $g(r)$ at different pinning concentrations. Without pinning, $g(r)$ shows regularly spaced peaks, indicating that the system is an ordered crystal, which is similar to the previous work.[21] As ρ_{pinning} increases, the regularly spaced peaks disappear gradually, confirming the loss of ordered structures and the formation of disorder structures [Fig. 1(e), main plot]. The first peak height of $g(r)$ decreases as ρ_{pinning} increases [Fig. 1(e), inset], clearly showing that the system structure changes from order to disorder.

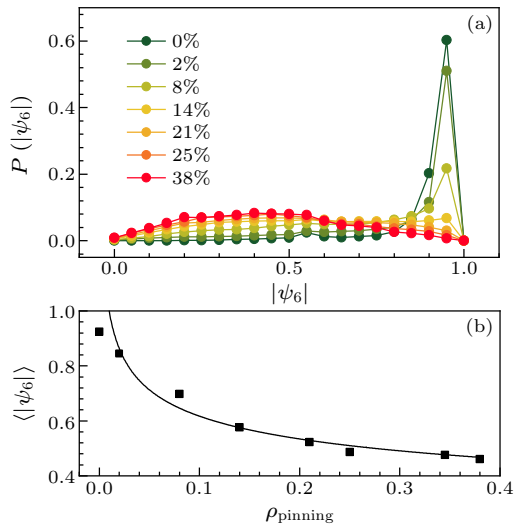

Fig. 2. (a) The probability distribution of the value of ψ_6 at different ρ_{pinning}. (b) The value of ψ_6 averaged over all particles versus ρ_{pinning}. The solid line is a power law fit.

To further capture the structure evolution, the ordering of each particle is analyzed, which is characterized by the bond orientational order parameter:[22,23] $\psi_{6j} = \frac{1}{\text{CN}}\sum_{k=1}^{\text{CN}} e^{i6\theta_{jk}}$, where CN is the coordination number of particle j and θ_{jk} is the angle of the bond between particle j and its neighbor k. Note that for perfect triangular lattices the value of the bond orientational order parameter is 1, and the decrease of the value demonstrates that the structure becomes disorder. The probability distribution of the value of $|\psi_6|$ is shown in Fig. 2(a). In the absence of pinning, a distinct peak is observed at a large value, indicating the dominated ordered structures. As ρ_{pinning} increases, the height of the peak decreases and the position of the peak shifts to small $|\psi_6|$. This signifies that the system transforms into the disordered structures with increasing ρ_{pinning}. The disordering transition is directly reflected by the value of ψ_6 averaged over all particles ($\langle|\psi_6|\rangle$) shown in Fig. 2(b). As ρ_{pinning} increases, $\langle|\psi_6|\rangle$ exhibits a power law decay. The decrease of $\langle|\psi_6|\rangle$ confirms that there are more defects in the system with increasing ρ_{pinning}, which induce the order-to-disorder transition. This is consistent with the results obtained from the Voronoi diagram and the pair correlation function (Fig. 1).

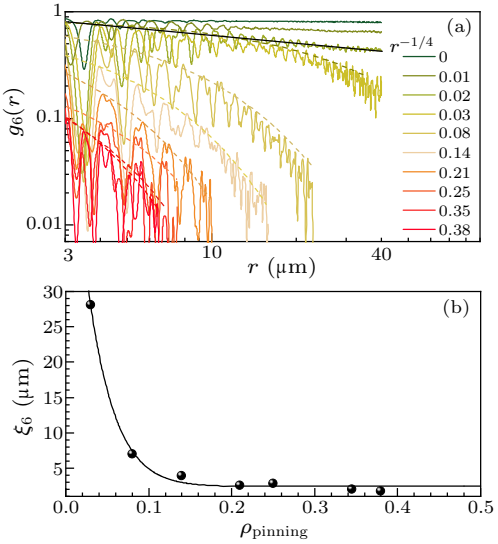

Fig. 3. (a) Spatial correlation function $g_6(r)$ of the bond orientational order parameter at different fractions of pinning (from top to bottom): $\rho_{\text{pinning}} = 0$, 0.01, 0.02, 0.03, 0.08, 0.14, 0.21, 0.25, 0.35, 0.38. Here $r^{-1/4}$ (solid line) is the KTHNY prediction at the quasi-long-range orientational order to short-range orientational order transition point. The dashed curves are fits of $g_6(r)$ to e^{-r/ξ_6}. (b) The orientational correlation length ξ_6 obtained from the fits in (a). The solid curve is a fit to the $\xi_6 \propto e^{b/\sqrt{|\rho_c - \rho_{\text{pinning}}|}}$ with $\rho_c = 0.02$, the hallmark of the KTHNY theory.

Moreover, to elucidate the spatial range of the structural ordering, the orientational correlation function is calculated: $g_6(r = |\boldsymbol{r}_i - \boldsymbol{r}_j|) = \langle\psi_{6i}^*(\boldsymbol{r}_i)\psi_{6j}(\boldsymbol{r}_j)\rangle$, where $\boldsymbol{r}_i$ and $\boldsymbol{r}_j$ are the positions of particles i and j, respectively. Without pinning, $g_6(r)$ is nearly constant, indicating that the system is in a crystal phase with long-range orientational order [Fig. 3(a)]. At $\rho_{\text{pinning}} = 0.01$ and 0.02, $g_6(r)$ decays algebraically, suggesting that the system is in hexatic phase with quasi-long-range orientational order. At high ρ_{pinning}, $g_6(r)$ decays exponentially, indicating that the system transforms from quasi-long-range orientational order to short-range orientational order [Fig. 3(a)]. This is a direct structural evidence of the crystal-hexatic-glass transition, similar to that in crystal-hexatic-liquid transition. The orientational correlation length ξ_6 is obtained from the fits of $g_6(r)$ to e^{-r/ξ_6}. As ρ_{pinning} increases, ξ_6 decreases. It is noticed that ξ_6 exhibits a critical be-

havior, $e^{b/\sqrt{|\rho_c-\rho_{\rm pinning}|}}$,[24] and the critical point of the crystal-to-glass transition is obtained, $\rho_c = 0.02$ [Fig. 3(b)]. The critical behavior is the hallmark of the KTHNY theory, and the critical point is consistent with the direct observation of the transformation from quasi-long-range orientational order to short-range orientational order, at which $g_6(r)$ exhibits $r^{-1/4}$ [see the solid line in Fig. 3(a)], in agreement with the KTHNY predictions.

The above analysis of the structural properties only directly verifies the order-to-disorder structure transition. To prove that the state after the structure transition is a glass phase at high pinning fraction, the dynamics of the system is investigated. Figure 4(a) shows the mean square displacement (MSD)[25] of non-pinning particles, $\langle \Delta r^2(t)\rangle = \langle |\boldsymbol{r}(t) - \boldsymbol{r}(0)|^2\rangle$, at different $\rho_{\rm pinning}$. Although there is an increase in the MSD after the order-to-disorder structure transition, a plateau without obvious rise within the experimental time window is observed at $\rho_{\rm pinning} = 0.08$, demonstrating that the particles are arrested in the cages formed by their near neighbors, which is a characteristic of the glass state. This confirms that the system enters into the glass phase rather than the liquid phase at high $\rho_{\rm pinning}$. Interestingly, with further increase of $\rho_{\rm pinning}$, an increase and then decrease of the MSD are observed. Specifically, at $\rho_{\rm pinning} = 0.14$ the MSD shows a significant increase at long times, which demonstrates that the particles have the ability to escape from the cages exhibiting the diffusion behavior. However, at $\rho_{\rm pinning} = 0.38$, the MSD decreases back, exhibiting a behavior similar to that at $\rho_{\rm pinning} = 0.08$.

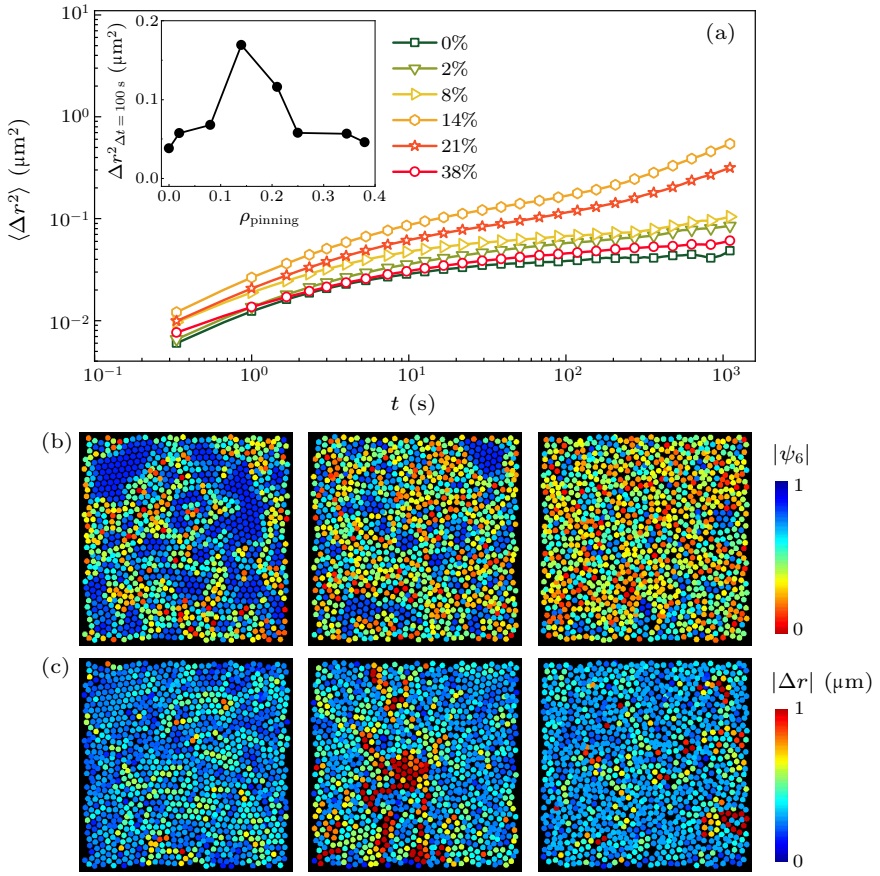

Fig. 4. (a) Mean square displacement of the moving particles, Δr^2, plotted against lag time, and Δr at $\rho_{\rm pinning} = 0$, 0.02, 0.08, 0.14, 0.21, 0.38. Inset: the value of Δr^2 for $\Delta r = 100$ s as a function of $\rho_{\rm pinning}$. (b) Representative spatial distributions of ψ_6 at $\rho_{\rm pinning} = 0.08$, 0.14 and 0.25 (from left to right). (c) The corresponding spatial distributions of particle displacements over a lag time of 500 s at $\rho_{\rm pinning} = 0.08$, 0.14 and 0.25 (from left to right). Note that the faster moving particles form clusters in the intermediate pinning fraction.

The inset in Fig. 4(a) clearly shows the non-monotonic dependence of the dynamics on $\rho_{\rm pinning}$. The enhancement of the dynamics with increasing $\rho_{\rm pinning}$ is suggested to originate from the destruction of the periodic crystalline structure due to the disorder [Fig. 4(b)], which thus decreases the energy barrier for the particle motions.[26–28] Therefore, the dynamics increases as the phase transition takes place, consistent with the same transition induced by particle polydispersity.[5] When $\rho_{\rm pinning}$ increases up to 0.14, it leads to more disorder corresponding to more faster dynamics [Figs. 4(b) and 4(c), medium panels], which thus causes the system to deviate from the deep arrest state. However, once $\rho_{\rm pinning}$ further increases, the confining character of the pinning becomes to dominate the dynamics, which thereby decreases the dynamics [Fig. 4(c), right panels] driving the system back to the deep arrest state.[29] Such a competition be-

tween the disorder that enhances the dynamics and the pinning that hinders the particle motions thereby leads to the non-monotonic change of the dynamics with increasing $\rho_{\rm pinning}$, which is similar to the previous work.[30]

The spatial distributions of the particle displacements in Fig. 4(c) indicate that heterogeneous dynamics is involved in the system. To quantify such dynamic heterogeneity, the four-point susceptibilities at different $\rho_{\rm pinning}$ are calculated: $\chi_4(a,\Delta t) = N(\langle Q_2(a,\Delta t)^2\rangle - \langle Q_2(a,\Delta t)\rangle^2)$, where $Q_2 = \frac{1}{N}\sum_{i=1}^{N}\exp(-\Delta r^2/2a^2)$, a is the pre-selected length scale to be probed and Δr_i is the distance particles i moves in time Δt. Here χ_4 is small and flat at $\rho_{\rm pinning} = 0$, as expected for a homogeneous dynamics for crystal phase. With increasing $\rho_{\rm pinning}$, χ_4 exhibits a peak, indicating that the heterogeneous dynamics appears (Fig. 5, main plot), consistent with the precious work during the crystal-to-glass transition.[5] As $\rho_{\rm pinning}$ increases up to 0.14, χ_4 reaches the maximum (Fig. 5, inset) indicating the strongest dynamic heterogeneity. This is consistent with the existence of the cooperative motions of the particles in the system, reflected by the clusters of the fast moving particles [see the red particles in Fig. 4(c), medium panel].[31–33] However, as $\rho_{\rm pinning}$ continues to increase ($\rho_{\rm pinning} > 0.14$), χ_4 decreases, signifying that the dynamic heterogeneity decreases, which is similar to that found in the simulation of pinning systems.[12] It is argued that such pinning-induced dynamics is due to the fact that the moving particles are hindered by the pinning particles, leading to homogeneous confined motions.[6,8,12]

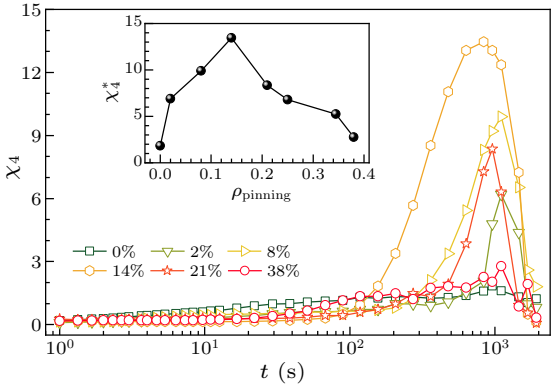

Fig. 5. The four-point susceptibility χ_4 is plotted versus Δt, at $\rho_{\rm pinning} = 0$, 0.02, 0.08, 0.14, 0.21, 0.38, with probing length scale a, chosen to maximize the peak in χ_4. Inset: the maximum value of χ_4, i.e., χ_4^*, plotted versus $\rho_{\rm pinning}$.

In conclusion, we have, for the first time, found a crystal-hexatic-glass transition due to the presence of disorder induced by random pinning. Such glass formation from crystal is different from the liquid-to-glass transition since the transition can be characterized by both the structural signatures and the dynamics properties. Moreover, the results reveal an interesting non-monotonic change of the dynamics with increasing pinning density, which calls for the theoretical study in the future. Our work uncovers one of the key roles of pinning on phase transitions in colloidal systems, and demonstrates a novel experimental strategy to form glass and to understand the glass transition.

References

[1] Nelson D R and Halperin B I 1979 *Phys. Rev. B* **19** 2457
[2] Tamborini E, Royall C P and Cicuta P 2015 *J. Phys.: Conden. Matter* **27** 194124
[3] Vanblaaderen A and Wiltzius P 1995 *Science* **270** 1177
[4] Ediger M D, Angell C A and Nagel S R 1996 *J. Phys. Chem.* **100** 13200
[5] Yunker P, Zhang Z X and Yodh A G 2010 *Phys. Rev. Lett.* **104** 015701
[6] Kim K, Miyazaki K and Saito S 2009 *Europhys. Lett.* **88** 36002
[7] Kob W and Berthier L 2013 *Phys. Rev. Lett.* **110** 245702
[8] Kim K, Miyazaki K and Saito S 2011 *J. Phys.: Conden. Matter* **23** 234123
[9] Hocky G M, Berthier L and Reichman D R 2014 *J. Chem. Phys.* **141** 224503
[10] Cammarota C and Biroli G 2012 *Proc. Natl. Acad. Sci. USA* **109** 8850
[11] Cammarota C 2013 *Europhys. Lett.* **101** 56001
[12] Kob W and Coslovich D 2014 *Phys. Rev. E* **90** 052305
[13] Han Y, Ha N Y, Alsayed A M and Yodh A G 2008 *Phys. Rev. E* **77** 041406
[14] Gokhale S, Nagamanasa K H, Ganapathy R and Sood A K 2014 *Nat. Commun.* **5** 4685
[15] Liu L L, Kheifets S, Ginis V, Di Donato A and Capasso F 2017 *Proc. Natl. Acad. Sci. USA* **114** 11087
[16] Yada M, Yamamoto J and Yokoyama H 2004 *Phys. Rev. Lett.* **92** 185501
[17] Crocker J C, Matteo J A, Dinsmore A D and Yodh A G 1999 *Phys. Rev. Lett.* **82** 4352
[18] Israelachvili J N 2011 *Intermolecular and Surface Forces* 3nd edn (New York: Academic Press)
[19] Zheng Z and Han Y 2010 *J. Chem. Phys.* **133** 124509
[20] Crocker J C and Grier D G 1996 *J. Colloid Interf. Sci.* **179** 298
[21] Sun X Y, Li Y, Zhang T H, Ma Y Q and Zhang Z X 2013 *Langmuir* **29** 7216
[22] Zhou C C, Shen H C, Tong H, Xu N and Tan P 2020 *Chin. Phys. Lett.* **37** 086301
[23] Shen H C, Tong H, Tan P and Xu L 2019 *Nat. Commun.* **10** 1737
[24] Nelson D R 2002 *Defects and Geometry in Condensed Matter Physics* (Cambridge: Cambridge University Press)
[25] Tong H and Xu N 2014 *Phys. Rev. E* **90** 010401
[26] Nabarro F R N 1987 *Theory of Crystal Dislocations* (Oxford: Oxford Clarendon Press)
[27] Pertsinidis A and Ling X S 2001 *Phys. Rev. Lett.* **87** 098303
[28] Chen Y, Tan X L, Wang H G, Zhang Z X, Kosterlitz J M and Ling X S 2021 *Phys. Rev. Lett.* **127** 018004
[29] Liu J, Tong H, Nie Y H and Xu N 2020 *Chin. Phys. B* **29** 126302
[30] Deutschländer S, Horn T, Löwen H, Maret G and Keim P 2013 *Phys. Rev. Lett.* **111** 098301
[31] Ediger M D 2000 *Annu. Rev. Phys. Chem.* **51** 99
[32] Eral H B, Mugele F and Duits M H 2011 *Langmuir* **27** 12297
[33] Zhang Z X, Yunker P J, Habdas P and Yodh A G 2011 *Phys. Rev. Lett.* **107** 208303

Supplementary Material for "Observation of the Pinning-Induced Crystal-Hexatic-Glass Transition in Two-Dimensional Colloidal Suspensions"

Xiao-Yan Sun (孙晓燕)[1,#], Hua-Guang Wang(王华光) [2,#], Hao Feng(冯浩)[3], Ze-Xin Zhang(张泽新)[2,3,**], and Yu-Qiang Ma(马余强)[4,**]

[1]Department of Optoelectronics and Energy Engineering, City College of Suzhou, Suzhou 215104, PR China

[2]College of Chemistry, Chemical Engineering and Materials Science, Soochow University, Suzhou 215123, PR China

[3]Center for Soft Condensed Matter Physics and Interdisciplinary Research, Soochow University, Suzhou 215006, PR China

[4]National Laboratory of Solid State Microstructures and Department of Physics, Nanjing University, Nanjing 210093, PR China

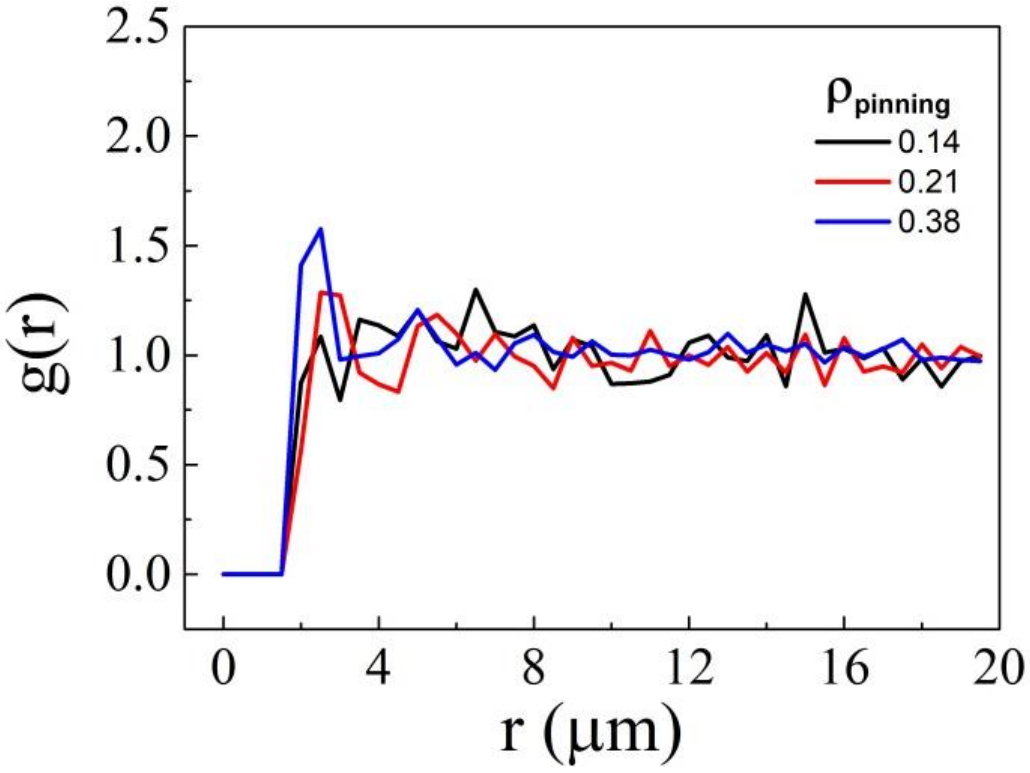

Fig. S1 g(r) of pinning particles at different pinning concentrations, $\rho_{pinning}$.

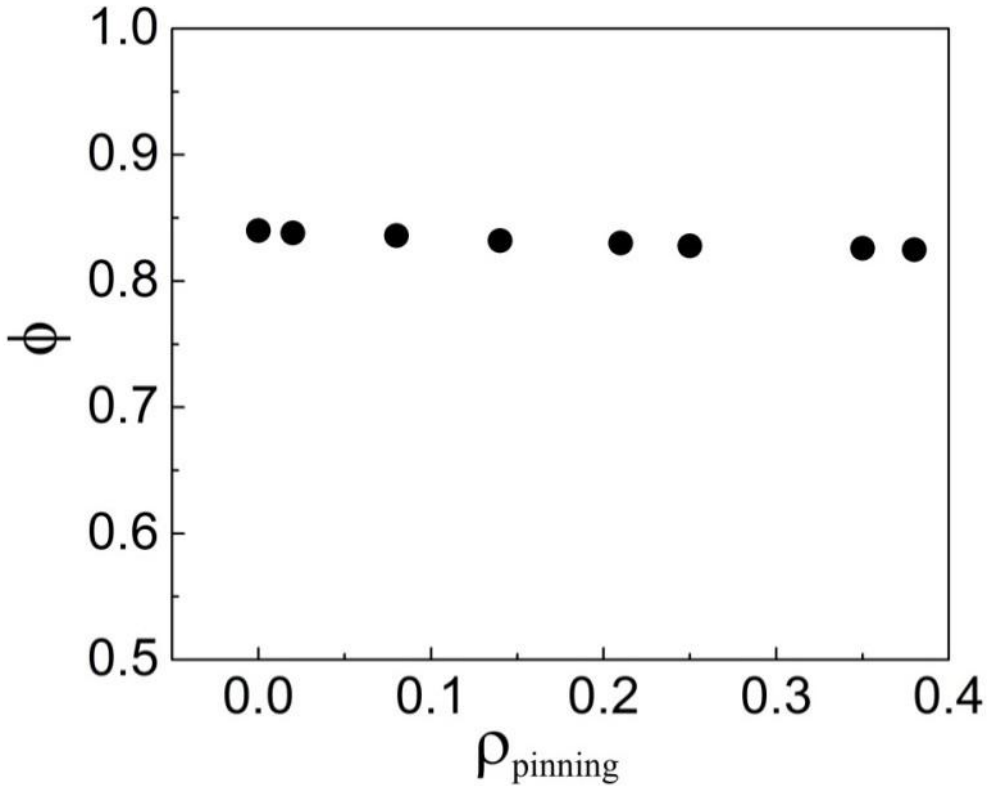

Fig. S2 The area fraction vs. pinning concentration, $\rho_{pinning}$.